IOP Conf. Series: Journal of Physics: Conf. Series **868** (2017) 012007 doi:10.1088/1742-6596/868/1/012007

Quasi-two-dimensional magnetism in Cr-based MAX phases

Takeshi Waki, Zhongsheng Liu, Yoshikazu Tabata and Hiroyuki Nakamura

Department of Materials Science and Engineering, Kyoto University, Kyoto 606-8501, JAPAN

E-mail: waki.takeshi.5c@kyoto-u.ac.jp

Abstract. The MAX phase is one possible candidate for quasi-two-dimensional (Q2D) magnets owing to its layered structure. We report itinerant electron ferromagnetic and antiferromagnetic long-range orders in $(Cr_{1-x}Mn_x)_2GeC$ and Cr_2GaN, respectively. Because Cr_2GaN orders in a spin-density-wave state, the Q2D character is highly plausible. However, the Q2D nature is not straightforward in $(Cr_{1-x}Mn_x)_2GeC$ because of the absence of useful criteria to judge the dimensionality in the itinerant electron ferromagnet. In this article, we attempt to reveal the Q2D character of ferromagnetic $(Cr_{1-x}Mn_x)_2GeC$ by analyzing magnetic data in terms of the spin fluctuation theory for the Q2D system.

1. Introduction

Quasi-two-dimensional (Q2D) itinerant electron magnets have been attracting a great deal of attention in condensed matter physics research. Particularly, unconventional superconductivity in Q2D materials is one of the most familiar examples. A superconducting phase is often found in the vicinity of a magnetically ordered phase of layered materials such as cuprates and iron pnictides.

We have focused on the MAX phase as a new candidate for a Q2D itinerant electron magnet. The chemical formula of the MAX phase is $M_{n+1}AX_n$, where M is an early transition metal, A is a main group metal, X is carbon or nitrogen, and n = 1, 2, 3. The $M_{n+1}X_n$ layer and the A triangular lattice layer are piled up alternatively to form the layered structure [1]. Although the known stable phases were found in the 1960s–70s [2], the magnetism of the MAX phase has remained almost unexplored. Among stable MAX phases, only Cr-based materials are likely to be magnetic. We first surveyed the magnetism of nondoped Cr-base materials Cr_2AlC, Cr_2GaC, Cr_2GeC, and Cr_2GaN and found that the carbides are all Pauli paramagnetic, whereas Cr_2GaN shows a spin-density-wave (SDW) transition at 170 K [3]. As far as we know this is the only example of the bulk nondoped magnetically ordered MAX phase. However, room temperature ferromagnetism in a $(Cr_{0.75}Mn_{0.25})_2GeC$ thin film has been reported [4]. Independently, we confirmed bulk ferromagnetism and its systematic enhancement in the $(Cr_{1-x}Mn_x)_2GeC$ system [5].

The Q2D magnetism in localized spin systems is often discussed based on the magnetic susceptibility χ. Deviation from the Curie-Weiss law and a broad maximum in χ at a low temperature associated with magnetic short-range order are signatures of Q2D magnetism. In the itinerant electron case, the appearance of the SDW state suggests strongly Q2D

antiferromagnetism because it often originates from the low-dimensional nature of the Fermi surfaces and their nesting. This is the case of Cr_2GaN. However, it is difficult to discuss the Q2D character in $(Cr_{1-x}Mn_x)_2GeC$ because of the absence of established criteria for the itinerant electron ferromagnet.

Spin fluctuation parameters, which can be estimated from macroscopic magnetic data using Takahashi's spin fluctuation theory [6], would be helpful to discuss Q2D itinerant electron ferromagnetism. Recently, spin fluctuation parameters were estimated for itinerant electron ferromagnets with layered structures [7, 8, 9, 10, 11, 12]. In the generalized Rhodes-Wohlfarth plot, some systems exhibit significant deviation from the three-dimensional (3D) theoretical relation. However, it is difficult to judge whether the deviation is due to low dimensionality.

In this article, as a more quantitative discussion for the systematic deviation from the 3D line for $(Cr_{1-x}Mn_x)_2GeC$, we analyzed macroscopic magnetic data using Takahashi's spin fluctuation theory [6] and its extension to the Q2D system [13].

2. Experiments

Polycrystalline samples of $(Cr_{1-x}Mn_x)_2GeC$ were synthesized by solid state reaction of powder elements in evacuated quartz silica tubes. The heating temperature was 950–1000°C. Macroscopic magnetic measurements were performed using a SQUID magnetometer (MPMS, Quantum Design) at T = 2–300 K and H = 0–7 T.

3. Analysis

Here we describe the analysis used to estimate spin fluctuation parameters and the index of dimensionality using magnetization data.

Wave number and frequency dependencies of the imaginary part of the dynamical susceptibility for weak itinerant electron ferromagnets can be described by a double Lorentzian spectrum. As measures of spectral widths in wave-vector and energy spaces, T_A and T_0 are introduced, respectively [14].

On the other hand, Landau's expansion of the magnetic free energy at the ground state is described as

$$F_{\rm m}(M) = F_{\rm m}(0) + \frac{1}{2(g\mu_{\rm B})^2\chi}M^2 + \frac{\bar{F}_1}{4(g\mu_{\rm B})^4 N_0^3}M^4, \tag{1}$$

where g is the Lande's g-factor, χ is the magnetic susceptibility, $\mu_{\rm B}$ is the Bohr magneton and N_0 is the number of magnetic ions. $\bar{F}_1$ corresponds to the slope of the Arrott plot. Experimentally we can estimate $\bar{F}_1$ with the relation as

$$\bar{F}_1 = \frac{N_0^3(2\mu_{\rm B})^4}{\xi k_{\rm B}}, \tag{2}$$

where ξ is the slope of the Arrott plot at zero temperature and $k_{\rm B}$ is the Boltzmann constant.

In Takahashi's spin fluctuation theory, $\bar{F}_1$ is related to T_A and T_0 as

$$\bar{F}_1 = \frac{4T_A^2}{15T_0}. \tag{3}$$

We also obtain the relation among the spontaneous moment at the ground state $p_{\rm s}$, T_A and T_0 as

$$p_{\rm s}^2 = \frac{20T_0}{T_A}C_{4/3}\left(\frac{T_{\rm C}}{T_0}\right)^{4/3}, \tag{4}$$

where $C_{4/3}$=1.00608$\cdots$. Using Eqs.(3) and (4), we can estimate T_A and T_0 from macroscopic magnetic data.

Takahashi's spin fluctuation theory is extended to the Q2D system by introducing the anisotropy to the electron effective mass. As a measure of the dimensionality, $\epsilon^2 = m/m'$ is used, where m and m' are the effective in-plane and out-of-plane components of the mass, respectively. In this treatment, the relation among $\bar{F}_1$, T_A and T_0 can be modified from the 3D case as

$$\bar{F}_1 = \frac{2T_A^2}{5d_z T_0}, \qquad d_z = \frac{6-3\epsilon}{3-\epsilon^2}. \tag{5}$$

As a result, we obtain, for the Q2D case, the relations

$$\left(\frac{T_{\rm C}}{T_A}\right)^{5/3} = \frac{p_{\rm s}^2}{5g^2 C_{4/3}} \left(\frac{5d_z\bar{F}_1}{2T_{\rm C}}\right)^{-1/3} \tag{6}$$

and

$$\left(\frac{T_{\rm C}}{T_0}\right)^{5/6} = \frac{p_{\rm s}^2}{5g^2 C_{4/3}} \left(\frac{5d_z\bar{F}_1}{2T_{\rm C}}\right)^{1/2} \tag{7}$$

which enable us to calculate the spin fluctuation parameters using macroscopic data. When we calculate T_A and T_0 using these equations, ϵ should be set in addition to macroscopic magnetic data. To estimate ϵ, we use the generalized Rhodes-Wohlfarth plot.

Although the original Rhodes-Wohlfarth plot was proposed empirically, Takahashi showed that $p_{\rm eff}/p_{\rm s}$ plotted against $T_{\rm C}/T_0$ satisfies

$$\frac{p_{\rm eff}}{p_{\rm s}} = 1.4\left(\frac{T_{\rm C}}{T_0}\right)^{-2/3} \tag{8}$$

for a 3D itinerant electron weak ferromagnet. For the Q2D case, the relation between $p_{\rm eff}/p_{\rm s}$ and $t_{\rm c} = T_{\rm C}/T_0$ is given as a function of ϵ as

$$\left(\frac{p_{\rm eff}}{p_{\rm s}}\right)^2 = \frac{3}{10d_T t_{\rm c} T(t_{\rm c},\epsilon)} \left(\frac{dy}{dt}\right)^{-1}, \tag{9}$$

with

$$d_T = \frac{6}{3-\epsilon^2}, \quad t_{\rm c}T(t_{\rm c},\epsilon) = \epsilon^3\Big(H_{\rm 3D}(0,t_{\rm c},\epsilon) + H_{\rm 2D}(0,t_{\rm c},\epsilon)\Big), \tag{10}$$

$$y = \frac{N_0(g\mu_{\rm B})^2}{2k_{\rm B}T_A\chi}, \tag{11}$$

$$y = \frac{\epsilon^3}{1-\epsilon/2}\bigg(\Big(H_{\rm 3D}(y,t,\epsilon) + H_{\rm 2D}(y,t,\epsilon)\Big) - \Big(H_{\rm 3D}(0,t_{\rm c},\epsilon) + H_{\rm 2D}(0,t_{\rm c},\epsilon)\Big)\bigg), \tag{12}$$

$$H_{\rm 3D}(y,t,\epsilon) = \int_0^1 z^3 dz \left(\ln\nu - \frac{1}{2\nu} - \psi(\nu)\right), \tag{13}$$

$$H_{\rm 2D}(y,t,\epsilon) = \int_1^{1/\epsilon} z^2 dz \left(\ln\nu - \frac{1}{2\nu} - \psi(\nu)\right), \tag{14}$$

$$t = \frac{T}{T_0}, \quad \eta = y/\epsilon^2, \quad \tau = t/\epsilon^3, \quad \nu = z(\eta+z^2)/\tau, \tag{15}$$

where $\psi(\nu)$ is the digamma function. In contrast ot the 3D case, the theoretical relation for the Q2D case needs numerical calculations, because Eq.(9) is not analytic. Calculated curves deviate downward from the 3D line (Eq.(8)) with decreasing ϵ. By using these curves we can estimate ϵ for the data points. Since the location of the data points in the plot depends on the presumed ϵ value to calculate T_0, ϵ should be determined self-consistently.

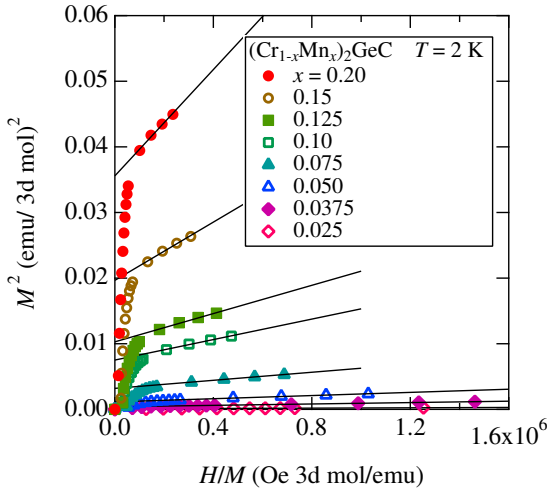

Figure 1. Arrott plot for $(Cr_{1-x}Mn_x)_2GeC$ at $T = 2$ K. Solid lines indicate the best fits for different concentration data.

4. Results and Analysis

Figure 1 shows the Arrott plot for $(Cr_{1-x}Mn_x)_2GeC$ at $T = 2$ K. Since the T_C values of $(Cr_{1-x}Mn_x)_2GeC$ are sufficiently high compared to 2 K, we estimate p_s and F_1 from these data by regarding the magnetization as that of the ground state. Solid lines are the best fits of the data to

$$M^2 = p_s^2 + \xi \frac{H}{M}. \tag{16}$$

With increasing x, the M^2-intercept or p_s increases monotonically. The slope also increases, suggesting that changes in the spin fluctuation are associated with the Mn substitution.

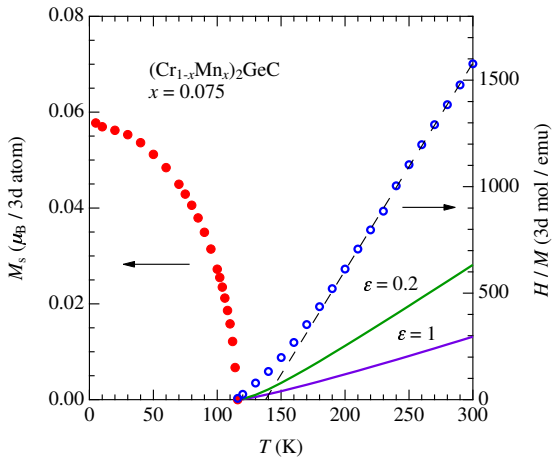

Figure 2. Temperature dependence of magnetization and reciprocal susceptibility for $x = 0.075$ estimated from the Arrott plot. The solid circles represent the temperature dependence of $M_s(T)$ (left axis). Open circles represent reciprocal susceptibility (right axis). The dashed line is the best fit to the Curie-Weiss law. Solid curves represent calculated reciprocal susceptibility for $\epsilon = 0.2$ and 1.

In Fig. 2, the temperature dependence of the spontaneous moment $M_s(T)$ estimated from the Arrott plot is shown for $x = 0.075$. With increasing temperature, $M_s(T)$ decreases monotonically to be zero at $T_C = 115$ K. The magnetic susceptibility estimated from the Arrott plot was fitted with the modified Curie-Weiss law

$$\chi(T) = \frac{N_0 p_{\rm eff}^2 \mu_B^2}{3k_B(T-\theta)} + \chi_0, \tag{17}$$

where θ and χ_0 are the Weiss temperature and temperature independent susceptibility, respectively. The obtained parameters are $p_{\rm eff} = 0.888$ μ_B, $\theta = 138$ K, and $\chi_0 = 0.00019$

emu/mol. We show the temperature dependent term of the reciprocal susceptibility to compare it to the theoretical curves.

Table 1. Magnetic data and spin fluctuation parameters for $(Cr_{1-x}Mn_x)_2GeC$. To calculate T_A-Q2D and T_0-Q2D, we used the Q2D index $\epsilon = 0.2$. T_0-Q2D was used to calculate T_C/T_0.

x	T_C (K)	p_{eff} (μ_B)	p_s (μ_B)	$\bar{F}_1$ (10^4 K)	T_A-3D (10^4 K)	T_A-Q2D (10^4 K)	T_0-3D (10^4 K)	T_0-Q2D (10^4 K)	p_{eff}/p_s	T_C/T_0 10^{-3}
0.025	43	0.456	0.00961	831	102	106	3.31	2.94	47.5	1.46
0.0375	48	0.596	0.0197	201	35.2	36.6	1.62	1.44	30.2	3.30
0.050	75	0.712	0.0335	88.2	22.6	23.5	1.54	1.37	21.2	5.47
0.075	115	0.888	0.0566	35.2	14.1	14.7	1.51	1.34	15.7	8.56
0.10	150	1.15	0.0867	13.8	8.68	9.02	1.46	1.30	13.3	11.6
0.125	193	1.18	0.101	9.99	8.25	8.58	1.82	1.62	11.6	11.9
0.15	205	1.33	0.140	4.84	5.08	5.28	1.42	1.26	9.47	16.2
0.20	270	1.47	0.189	2.65	3.93	4.09	1.55	1.38	7.82	19.5

The magnetic data obtained are listed in Table 1. When we assume a 3D nature, T_A and T_0 can be readily calculated from these values. Even if we assume a 3D nature, the data for $(Cr_{1-x}Mn_x)_2GeC$ plotted in the form of $\log(p_{eff}/p_s)$ vs. $\log(T_C/T_0)$ are systematically shifted downward from the 3D line [5].

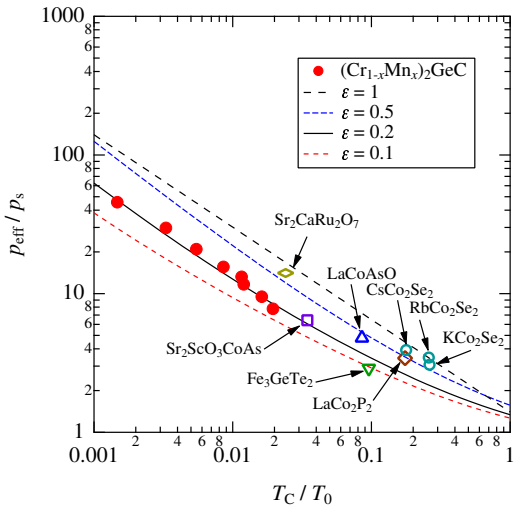

Figure 3. Generalized Rhodes-Wohlfarth plot for $(Cr_{1-x}Mn_x)_2GeC$. Theoretical curves for 3D and Q2D cases are drawn. Data points for $Sr_2CaRu_2O_7$ [7], LaCoAsO [8], Fe_3GeTe_2 [9], Sr_2ScO_3CoAs [10] ACo_2Se_2 (A = K, Rb, Cs) [11] and $LaCo_2P_2$ [12] are also included.

If we take into account ϵ, the data points slightly move to the right from the 3D case. As shown in Fig. 3, all the experimental data agree well with the case for $\epsilon = 0.2$, suggesting that $(Cr_{1-x}Mn_x)_2GeC$ are Q2D itinerant electron weak ferromagnets and that the dimensionality of this series is insensitive to the Mn content. The latter is consistent with the fact that lattice constants are almost independent of x [5]. The obtained ϵ value implies that the out-of-plane component of the effective mass is about 25 times larger than that of the in-plane one. To check the validity of the analysis, experimental estimation of the effective mass would be helpful.

In the figure, we add the data taken from the literature for other itinerant electron weak ferromagnets with layered structures. Although ϵ is not included when T_0 is estimated for these materials, some of the data points show an apparent downward deviation from the 3D

line, suggesting a Q2D character. This plot would be useful to estimate the dimensionality for itinerant electron ferromagnets.

Using Eqs.(11) and (12), we calculated the reciprocal susceptibility for $x = 0.075$ for 3D ($T_A = 14.1 \times 10^4$ K, $T_0 = 1.51 \times 10^4$ K and $\epsilon = 1$) and Q2D ($T_A = 14.7 \times 10^4$ K, $T_0 = 1.34 \times 10^4$ K and $\epsilon = 0.2$) cases, which are shown in Fig. 2. The reciprocal susceptibility calculated for the 3D case is about 1/4 that of the experimental one. By taking into account the Q2D nature, the agreement between theory and experiments is improved but not satisfactorily. For further improvement of the theory, Q2D analyses for other layered systems are desired. We do not dare to estimate the spin fluctuation parameters and ϵ from the reciprocal susceptibility because they cannot be determined independently.

5. Summary

We analyzed macroscopic magnetic data of $(Cr_{1-x}Mn_x)_2GeC$ using the spin fluctuation theory for Q2D itinerant electron ferromagnets. We observed a systematic deviation from the theoretical 3D line in the generalized Rhodes-Wohlfarth plot, whose appearance indicates a Q2D character. The index of dimensionality for the $(Cr_{1-x}Mn_x)_2GeC$ series was estimated to be $\epsilon = 0.2$ from a comparison of the data points and the theoretical curve in the plot.

References

[1] Barsoum M W 2000 *Prog. Solid State Chem.* **28** 201–281
[2] Nowotny V H 1971 *Progr. Solid State Chem.* **5** 27–70
[3] Liu Z, Waki T, Tabata Y, Yuge K, Nakamura H and Watanabe I 2013 *Phys. Rev.* B **88** 134401
[4] Ingason A S, Mockuté A, Dahlqvist M, Magnus F, Olafsson S, Arnalds U B, Alling B, Abrikosov I A, Hjörvarsson B, Persson P Å and Rosen J 2013 *Phys. Rev. Lett.* **110** 195502
[5] Liu Z, Waki T, Tabata Y and Nakamura H 2014 *Phys. Rev.* B **89** 054435
[6] Takahashi Y 1986 *J. Phys. Soc. Jpn.* **55** 3553–3573
[7] Ikeda S, Maeno Y and Fujita T 1998 *Phys. Rev.* B **57** 978
[8] Ohta H and Yoshimura K 2009 *Phys. Rev.* B **79** 184407
[9] Chen B, Yang J, Wang H, Imai M, Ohta H, Michioka C, Yoshimura K and Fang M 2013 *J. Phys. Soc. Jpn.* **82** 124711
[10] Ohta H, Noguchi D, Nabetani K and Katori H A 2013 *Phys. Rev.* B **88** 094441
[11] Yang J, Chen B, Wang H, Mao Q, Imai M, Yoshimura K and Fang M 2013 *Phys. Rev.* B **88** 064406
[12] Imai M, Michioka C, Ueda H and Yoshimura K 2015 *Phys. Rev.* B **91** 184414
[13] Takahashi Y 1997 *J. Phys.: Condens. Matter* **9** 10359
[14] Takahashi Y and Moriya T 1985 *J. Phys. Soc. Jpn.* **54** 1592–1598